Structural and thermal properties of Eu₂Ga₁₁Sn₃₅

Cite as: J. Appl. Phys. 133, 095108 (2023); https://doi.org/10.1063/5.0119852 Submitted: 10 August 2022 • Accepted: 09 February 2023 • Published Online: 03 March 2023

🤟 Wilarachchige D. C. B. Gunatilleke, 匝 Mingjian Zhang, 匝 Winnie Wong-Ng, et al.







ARTICLES YOU MAY BE INTERESTED IN

Is contour integration essential? Alternatives for beginning physics students American Journal of Physics 91, 170 (2023); https://doi.org/10.1119/5.0084475

Hopf bifurcation in a nonlocal nonlinear transport equation stemming from stochastic neural

Chaos: An Interdisciplinary Journal of Nonlinear Science 27, 021101 (2017); https:// doi.org/10.1063/1.4976510

Rosalind Franklin's X-ray photo of DNA as an undergraduate optical diffraction experiment American Journal of Physics 86, 95 (2018); https://doi.org/10.1119/1.5020051





Structural and thermal properties of Eu₂Ga₁₁Sn₃₅

Cite as: J. Appl. Phys. **133**, 095108 (2023); doi: 10.1063/5.0119852 Submitted: 10 August 2022 · Accepted: 9 February 2023 · Published Online: 3 March 2023







Wilarachchige D. C. B. Gunatilleke, ¹ D Mingjian Zhang, ² Winnie Wong-Ng, ³ Peter Zavalij, ⁴ D Yu-Sheng Chen, ² and George S. Nolas^{1,a)} D

AFFILIATIONS

- ¹Department of Physics, University of South Florida, Tampa, Florida 33620, USA
- ²ChemMatCARS, University of Chicago, Argonne, Illinois 60439, USA
- Materials Measurement Laboratory, National Institute of Standards and Technology, Gaithersburg, Maryland 20899, USA
- ⁴Department of Chemistry, University of Maryland, College Park, Maryland 20742, USA

ABSTRACT

Clathrates have been reported to form in a variety of different structure types; however, inorganic clathrate-I materials with a low-cation concentration have yet to be investigated. Furthermore, tin-based compositions have been much less investigated as compared to silicon or germanium analogs. We report the temperature-dependent structural and thermal properties of single-crystal Eu₂Ga₁₁Sn₃₅ revealing the effect of structure and composition on the thermal properties of this low-cation clathrate-I material. Specifically, low-temperature heat capacity, thermal conductivity, and synchrotron single-crystal x-ray diffraction reveal a departure from Debye-like behavior, a glass-like phonon mean-free path for this crystalline material, and a relatively large Grüneisen parameter due to the dominance of low-frequency Einstein modes. Our analyses indicate thermal properties that are a direct result of the structure and composition of this clathrate-I material.

Published under an exclusive license by AIP Publishing. https://doi.org/10.1063/5.0119852

INTRODUCTION

Inclusion and open-framework compounds can generally be described as consisting of a "host" lattice formed by two or more constituents resulting in voids, or channels, within the lattice that can be occupied by other constituents or "guest" atoms or molecules. 1,2 The intermolecular guest-host forces are typically much weaker than the bonds forming the lattice framework in such compounds, and an understanding of the guest-host interactions remains of intense fundamental interest and is required for technological applications.3-10 Inorganic clathrates represent one example of such materials and continue to be of interest since the report of "glass-like" thermal conductivity for Sr₈Ga₁₆Ge_{30.} Over the past two decades, considerable evidence has been reported that correlates the thermal properties of these materials with their structural features. 4,11-30 Moreover, low thermal conductivity is of interest for thermoelectric and thermal barrier materials, as thermal management plays a key role in these applications of interest.^{2,31}

Although clathrate-I compounds have been known for almost five decades, 35,36 inorganic clathrate-I compositions with low-cation concentrations have not yet been investigated. Open-framework compounds such as clathrate-II compositions and skutterudites with low-cation concentrations have been reported to show a direct

correlation between thermal conductivity, κ , and cation concentration, with lower κ achieved by reducing the number of cations per unit cell. $^{37-45}$ Nevertheless, no such work exists for clathrate-I compositions. Furthermore, an understanding of the thermal properties of low-cation clathrate-I materials would advance the development of these materials for the technological applications indicated above. Herein, we report on the thermal properties of the low-cation tin-based inorganic clathrate-I Eu₂Ga₁₁Sn₃₅. Specifically, temperature-dependent thermal conductivity, heat capacity, and single-crystal synchrotron x-ray diffraction were employed. We demonstrate that the thermal properties are due to lattice anharmonicity as well as Eu dynamic disorder in this crystalline clathrate-I material. The Grüneisen parameter was evaluated to quantify the lattice anharmonicity and an estimate of the phonon mean-free path indicates strong scattering of the heat-carrying phonons.

EXPERIMENTAL METHODS

Single crystals of $Eu_2Ga_{11}Sn_{35}$ were grown from Sn flux. The Eu, Ga, and Sn high purity elements were loaded into a tungsten crucible that was then sealed inside a custom-designed stainless-steel vessel in a 1:2:12 atomic ratio. The vessel was itself sealed in a glass tube under vacuum and heated to 650 °C at a rate of 25 °C

a)Author to whom correspondence should be addressed: gnolas@usf.edu

per hour, held for 15 h and then slowly cooled to 450 °C at a rate of 10 °C per hour before cooling to room temperature. Shiny Eu₂Ga₁₁Sn₃₅ crystals were obtained from the flux. Initial singlecrystal x-ray diffraction (XRD) studies were collected using a Bruker Smart Apex II CCD diffractometer with a Mo $K\alpha$ $(\lambda = 0.71073 \text{ Å})$ source. 46 The structural properties are integral in investigating the thermal properties of this material; therefore, temperature-dependent single-crystal x-ray diffraction was conducted at the microdiffraction facility at the Advanced Photon Source of Argonne National Laboratory (APS). The structure was determined using the ChemMatCARS advanced crystallography facility at the APS. The data were collected using a Huber 3 circles diffractometer equipped with a Pilatus3X 1M (CdTe) detector with a kappa angle offset of 60°. The distance between the detector and the crystal was 130 mm and a total of 1440 frames were collected at two angle settings, ω -angles = -180° , Kappa = 0° and ω -angles = -180, Kappa = 30°. The data were collected with the φ -angle scanned over 360° using shutterless mode. Data integration was performed with the APEX II suite software and data reduction employed the SAINT v.8.32B and SADABS v.2013 programs that were part of the APEX suite.⁴⁷ Structure solution and refinement were carried out with SHELX software using the XPREP utility for space group determination, and the XS and XL programs for structure solution and refinement, respectively. The structure was solved by the direct method and refined on F2(SHELXTL). Temperature-dependent κ , resistivity, ρ , and isobaric heat capacity, Cp, measurements were performed using the thermal transport option (TTO) and heat capacity option (HC), respectively, on the physical property measurement system from Quantum Design (PPMS). Details regarding these measurements are included in the supplementary material. Variation in these measurements is less than 5%, from the data reported herein as well as previous measurements on other materials. Furthermore, by employing standards we calibrate transport data from the PPMS and typically

compare with that from our custom-built system 48 for temperatures above 15 K.

RESULTS AND DISCUSSION

Temperature-dependent single-crystal XRD refinement data are shown in Table I, as well as Tables S1.1-S6 of the supplementary material. The room temperature structure can be found in the Cambridge Crystallographic Data Center database, entry CCDC 2154399. Europium occupies both the 2a (Eu1) and 6d (Eu2) sites in a 1:3 ratio, respectively, with no observed split position for these sites while the framework is made up of Ga and Sn. Gallium occupies all three framework sites with a preferential occupancy at the 6c site, as is typical of clathrate-I compositions. Figure 1 shows the clathrate-I crystal structure and the crystal used for thermal measurements. Figure 2 shows temperature-dependent isotropic atomic displacement parameters (U_{iso}). From the slope of U_{iso} vs temperature for the Eu sites and the three framework sites, one can obtain the Einstein modes due to Eu and the Debye temperature, $\theta_{\rm D}$, respectively. Employing $U_{\rm iso} = k_{\rm B}T/m(2\pi v)^{2,54}$ Einstein temperature, $\theta_{\rm E}$, values of 63 and 40 K for Eu1 and Eu2, respectively, were obtained. Here, $k_{\rm B}$ is the Boltzmann constant, T is the absolute temperature, m is the mass of the atom, v is the frequency of the Einstein modes, and $\theta_E = hv/k_B$. The temperature-dependent U_{iso} values for the three different Ga/Sn sites were used to calculate θ_D , employing $U_{\rm iso} = 3h^2/(mk_{\rm B}\theta_{\rm D}4\pi^2)T_{\rm s}^{55}$ resulting in $\theta_{\rm D} = 213$ K.

As indicated above, the structural features and disorder associated with clathrate-I compositions have a direct effect on the thermal properties and κ , in particular. It is, therefore, of interest to investigate κ for Eu₂Ga₁₁Sn₃₅. We employed a phenomenological model that consisted of Rayleigh (τ_R), resonant scattering (τ_{res}), Umklapp scattering (τ_{\ge}), and tunnel states (τ_{TS}) terms together with a term that represents the lower limit of the mean-free path L_{min} ($\tau_{min} = L_{min}/\nu$). Figure 3 shows the temperature dependence of

TABLE I. Crystallographic and structure refinement data for Eu₂Ga₁₁Sn₃₅.^a

	298 K	120 K	60 K	20 K	10 K
Empirical formula	$Eu_{2.2(2)}Ga_{11}Sn_{35}$	$Eu_{2.1(2)}Ga_{11}Sn_{35}$	$Eu_{2.1(2)}Ga_{11}Sn_{35}$	$Eu_{2.1(2)}Ga_{11}Sn_{35}$	Eu _{2,1(2)} Ga ₁₁ Sn ₃₅
Formula weight	5258.42	5244.00	5244.00	5242.48	5238.67
Crystal system, space group	Cubic, Pm3n	Cubic, Pm3n	Cubic, Pm3n	Cubic, Pm3n	Cubic, Pm3n
Z	1	1	1	1	1
a (Å)	11.9497(5)	11.930(2)	11.9202(5)	11.9191(6)	11.9199(6)
$\rho_{\rm calc} ({\rm g cm}^{-3})$	5.117	5.124	5.136	5.137	5.136
Goodness-of-fit on F^2 (S)	1.156	1.343	0.858	0.898	0.932
Final <i>R</i> indexes $[I \ge 4\sigma(I)]$	0.0095	$0.0164 \ (I \ge 2\sigma \ (I))$	0.0090	0.0089	0.0097
wR_2	0.0216	$0.0288 \ (I \ge 2\sigma \ (I))$	0.0197	0.0205	0.0219
<i>U</i> _{iso} —Eu1 @ 2 <i>a</i>	0.0366(7)	0.0216(10)	0.0167(7)	0.0148(7)	0.0137(8)
U _{iso} —Eu2 @ 6d	0.0986(9)	0.0577(12)	0.0437(7)	0.0342(6)	0.0336(6)
U _{iso} —Sn1/Ga1 @ 16 <i>i</i>	0.015 30(11)	0.009 24(11)	0.006 79(10)	0.005 44(10)	0.005 42(11)
U _{iso} —Sn2/Ga2 @ 24k	0.005 80(10)	0.009 87(10)	0.007 31(9)	0.006 11(9)	0.006 03(10)
U _{iso} —Sn3/Ga3 @ 6c	0.0172(2)	0.001 14(2)	0.0091(2)	0.0079(2)	0.0076(2)

 $^{^{}a}R = \Sigma ||F_{o}| - |F_{c}||/\Sigma |F_{o}|$. $wR_{2} = [\Sigma w(F_{o}^{2} - F_{c}^{2})^{2}/\Sigma w(F_{o}^{2})^{2}]^{1/2}$, $w = 1/[\sigma^{2}(F_{o}^{2}) + (0.0080P)^{2} + 1.1504P]$, where $P = (F_{o}^{2} + 2F_{c}^{2})/3$, σ is the error; F_{o} and F_{c} are the observed and calculated structure factors, respectively. $S = [\Sigma w(F_{o}^{2} - F_{c}^{2})^{2}/(N_{ref} - N_{par})]^{1/2}$, where N_{ref} is the number of independent reflections and N_{par} is the number of parameters.

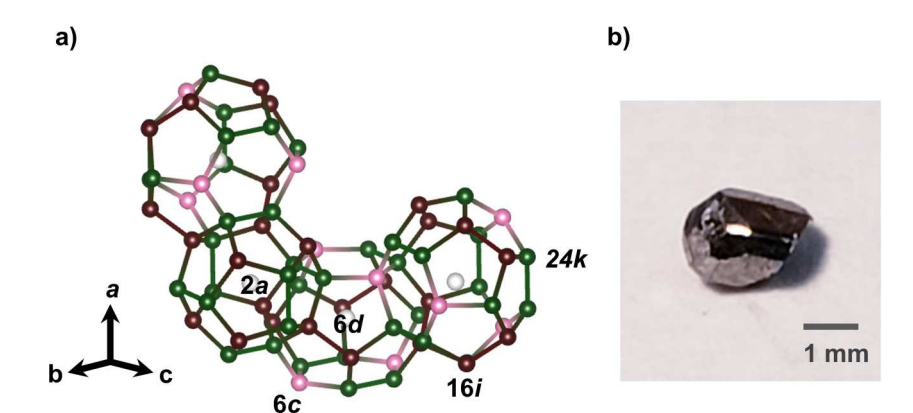


FIG. 1. (a) Clathrate-I crystal structure emphasizing the two polyhedra that form the framework, with the different Wyckoff sites labeled. (b) A picture of the Eu₂Ga₁₁Sn₃₅ crystal.

 κ together with the fit to the model, where the lattice contribution to κ , $\kappa_{\rm L}$, dominates the thermal conduction ($\kappa \approx \kappa_{\rm L}$) over the entire measured temperature range due to the high ρ values measured over the same temperature range (inset to Fig. 3). ⁵⁶

The fit employed the kinetic theory expression

$$\kappa_L = \frac{k_B}{2\pi^2 \nu} \left(\frac{k_B T}{\hbar}\right)^3 \int_0^{\theta_D/T} \frac{\tau_C x^4 e^x}{\left(e^x - 1\right)^2} dx,\tag{1}$$

with

$$\tau_C = (\tau_R^{-1} + \tau_{TS}^{-1} + \tau_{res}^{-1} + \tau_U^{-1})^{-1} + \tau_{\min}, \tag{2}$$

where

$$\tau_R^{-1} = A T^4 x^4, (3)$$

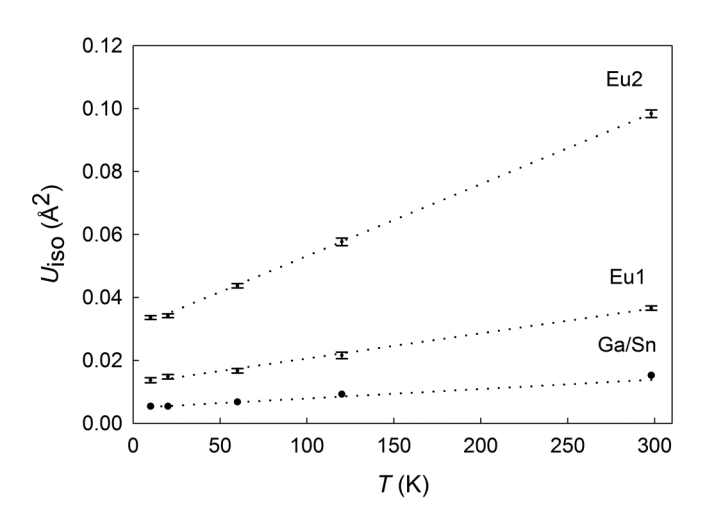


FIG. 2. Temperature-dependent $U_{\rm iso}$. The dotted lines for Eu1 and Eu2 represent linear data fits to the equation $U_{\rm iso}$ = $k_{\rm B}T/m(2\pi v)^2$. Only one representative data set for the framework Ga/Sn sites is shown due to the overlap in the data. The dotted line represents a linear data fit to the equation $U_{\rm iso}$ = $3h^2/(mk_{\rm B}\theta_{\rm D}4\pi^2)T$.

$$\tau_{TS}^{-1} = (BvxT) \tanh\left(\frac{xT}{2t}\right) + \left(\frac{Bv}{2}\right) \left(\frac{1}{xT} + C^{-1}T^{-3}\right)^{-1},$$
(4)

$$\tau_{res}^{-1} = \sum_{i} \frac{D_{i} x^{2} T^{4}}{(x_{i}^{2} - x^{2} T^{2})^{2} + g_{i} x_{i}^{2} x^{2} T^{2}},$$
 (5)

and

$$\tau_U^{-1} = UT^3 \exp\left(\frac{-\theta_D}{3T}\right) x^2. \tag{6}$$

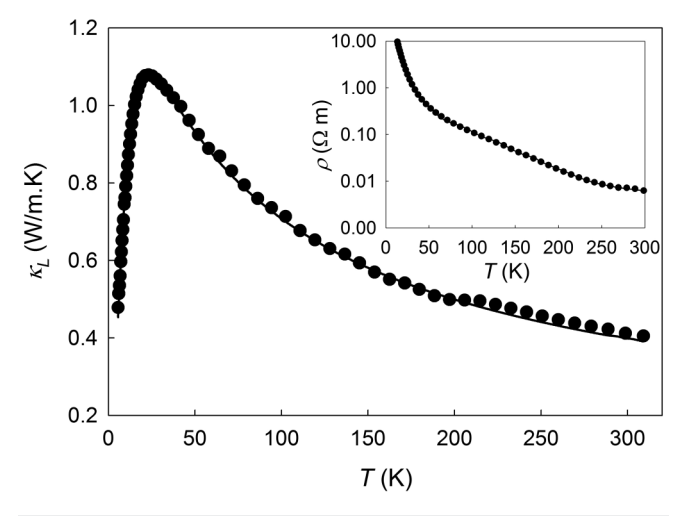


FIG. 3. Temperature-dependent κ_L . The solid line is the fit to the phenomenological model described in the text. The fit parameters obtained from the model were ν = 4000 ms⁻¹, L_{min} = 2.3 Å, A = 206 × 10⁻⁴³ s³, B = 3.96 × 10⁴ m⁻¹ K⁻¹, C = 0.02 K⁻², D_1 = 0.27 K⁻² s⁻³, D_2 = 0.77 K⁻² s⁻³, D_2/D_1 = 2.9, x_1 = 65 K, x_2 = 40 K, g_1 = 1.5, g_2 = 1.5, and U = 9.24 K⁻¹ s. The inset shows the temperature-dependent ρ for Eu₂Ga₁₁Sn₃₅. The high ρ values indicate intrinsic semiconducting behavior and an indication of the high quality of the crystal used for the low-temperature thermal measurements.

Here, $x = \hbar \omega / k_{\rm B} T$, v is the average speed of sound in the crystal lattice, ω_0 is the Einstein frequency, and the coefficients A, B, C, D_1 , D_2 , g_1 , g_2 , and U are fitting parameters related to the different phonon scattering processes. The fitting parameters were uniquely defined using a minimization of the best sequence fit function, as compared to the data, and all four terms were required to best fit the experimental data in the entire measured temperature range. The model resulted in an excellent fit to the data over the entire measured temperature range.

It is instructive to discuss specific findings from these results. First, although two resonances were used to account for Eu1 and Eu2, we found that this was also the minimum complexity required to best fit the data shown in Fig. 3. The fit to the data results in $\theta_{\rm E}$ values of 65 and 40 K for Eu1 and Eu2, respectively, in excellent agreement with that obtained from our structural data. In addition, the ratio D_2/D_1 (=2.9) is in accord with what is expected (\approx 3) for the ratio of the population of the two Eu Einstein modes and their relative scattering strengths. Moreover, the tunneling-state parameters are comparable to that of amorphous materials.⁵⁷ At very low temperatures (≤1 K), the dynamic disorder would necessarily "freeze-out," especially since adjacent cages to those containing Eu are empty due to the very low Eu concentration, resulting in more static disorder between Eu and the host framework that would presumably be characterized by a very small energy that separates these states.

Measurement and investigation of the heat capacity can also elucidate further on the above findings, as well as allow for estimates of phonon mean-free path and anharmonicity of the lattice. Figure 4 shows the C_P data. The inset to the figure shows a low-T fit employing a linear combination of the contributions to $C_P(=C_v=C_e(T)+C_{E1}(T)+C_{E2}(T)+C_D(T))$ used to fit the experimental data, where $C_e(T)$, $C_{E1}(T)$, $C_{E2}(T)$, and $C_D(T)$ are the electronic contribution, contributions from Einstein modes for Eu1 and Eu2, and the Debye contribution, respectively.

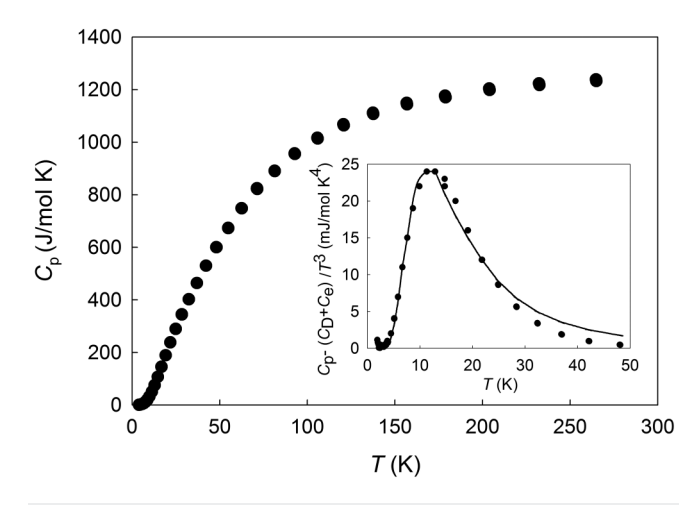


FIG. 4. Temperature-dependent $C_{\rm p}$. The inset shows the Einstein contribution to the heat capacity of Eu₂Ga₁₁Sn₃₅ with a solid line representing the data fit to the model described in the text.

The difference between C_p and the isochoric heat capacity, C_V , for Eu₂Ga₁₁Sn₃₅ is \leq 1% in the entire temperature range shown in Fig. 4. ^{58,59} The Einstein term is given by

$$C_{Ei}(T) = 3N_{Ei}R \left(\frac{\theta_{Ei}}{T}\right)^2 \frac{\exp\left(\frac{\theta_{Ei}}{T}\right)}{\left(\exp\left(\frac{\theta_{Ei}}{T}\right) - 1\right)^2},\tag{7}$$

and the Debye term by

$$C_D(T) = 9N_D R \left(\frac{T}{\theta_D}\right)^3 \int_0^{\theta_D/T} \frac{x^4 e^x}{(e^x - 1)^2} dx,$$
 (8)

where R is the molar gas constant, $N_{\rm Ei}$ is the number of Einstein oscillators i corresponding to the Einstein temperature $\theta_{\rm Ei}$ per formula unit, and $N_{\rm D}$ is the number of Debye oscillators per formula unit. For the data fit, $N_{\rm Ei}$, $\theta_{\rm Ei}$, and $\theta_{\rm D}$ were allowed to vary and $N_{\rm D}$ was assigned a fixed value of 46, which represents the number of framework atoms in the unit cell. From the parameters obtained from the fit $N_{\rm E2}/N_{\rm E1}$ = 2.5, reflecting the occupancy of Eu in each crystallographic site per unit cell, $\theta_D = 200 \text{ K}$, $\theta_{E1} = 65 \text{ K}$, and θ_{E2} = 57 K, all in very good agreement with values from our structural and κ data and analyses. The phonon mean-free path, L, can be estimated by utilizing $\kappa_L = (1/3)C_p vL$ together with the results and data described above. Figure 5 shows L as a function of temperature. Eu₂Ga₁₁Sn₃₅ has a shorter L than other clathrate-I compositions,60 presumably an indication that the combined dynamic disorder from Eu and static disorder from vacancies (vacant polyhedra) result in more efficient scattering of the heatcarrying phonons.

To gain insight into the anharmonicity of Eu₂Ga₁₁Sn₃₅, the Grüneisen parameter, γ , was estimated from $\gamma = \alpha_V KV/C_V$, where

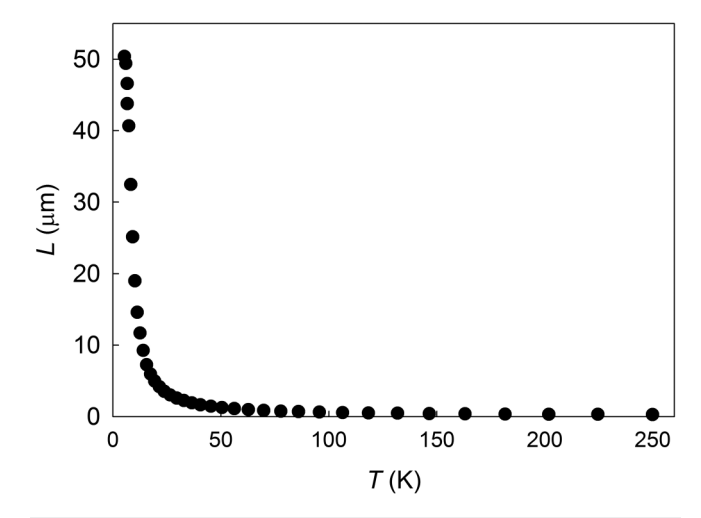


FIG. 5. Temperature-dependent phonon mean-free path, L, with L = 0.3 μ m above $\theta_{\rm D}$.

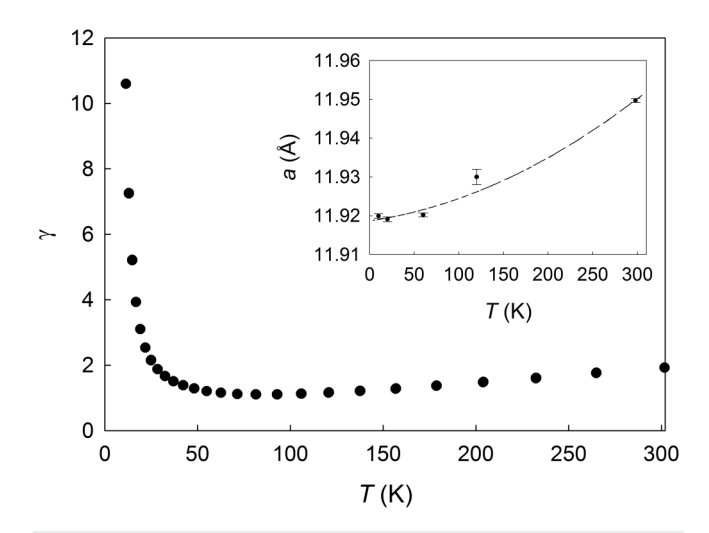


FIG. 6. Temperature-dependent average Grüneisen parameter. The inset shows the temperature-dependent lattice parameter for Eu₂Ga₁₁Sn₃₅. The dashed line represents a least square fit to the data for a polynomial of the form a (T) = a_0 + a_1 T + a_2 T² with values a_0 = 11.918, a_1 = 5.506 × 10⁻⁵ Å K⁻¹, a_2 = 1.711 × 10⁻⁷ Å K⁻² obtained from the fit. The obtained polynomial was used to estimate α_V using the expression α_V = (3/a(T)) da(T)/dT.

 $\alpha_{\rm V}$ is the volume expansion coefficient and $C_{\rm p} \approx C_{\rm V}$ for Eu₂Ga₁₁Sn₃₅.⁵⁹ Figure 6 shows the calculated γ vs T. The inset shows the temperature-dependent lattice parameters, a, that were used to calculate $\alpha_{\rm V}$. At room temperature, γ is relatively large but increases as the temperatures decrease at low temperatures. A similar trend has been observed in other clathrate-I compositions, including inorganic Na₈Si₄₆⁶⁰⁻⁶³ and clathrate hydrates, ^{64,65} as well as for other inclusion compounds, ^{66,67} and has been attributed to low-frequency modes. ^{60,66,67}

CONCLUSIONS

Temperature-dependent single-crystal structural and thermal properties of the low europium concentration tin clathrate-I Eu₂Ga₁₁Sn₃₅ were investigated. The relatively small europium inside the framework resulted in low-frequency Einstein modes as well as low thermal conductivity and a phonon mean-free path. This material also possesses anomalously large values of the Grüneisen parameters at low temperatures. Our results provide the foundation for an understanding of the thermal properties of very low-cation clathrate-I materials. Building on this work with theoretical calculations would be of interest in providing additional insight.

SUPPLEMENTARY MATERIAL

See the supplementary material for temperature-dependent structure refinement data for Eu₂Ga₁₁Sn₃₅.

ACKNOWLEDGMENTS

The authors acknowledge financial support from the U.S. National Science Foundation (NSF) under Grant No.

DMR-1748188. The authors thank B. Hyde for thermal conductivity PPMS measurements. ChemMatCARS Sector 15 was principally supported by the Divisions of Chemistry (CHE) and Materials Research (DMR), National Science Foundation, under Grant No. NSF/CHE-1834750. The use of the Advanced Photon Source, an Office of Science User Facility operated for the U.S. Department of Energy (DOE) Office of Science by Argonne National Laboratory, was supported by the U.S. DOE under Contract No. DE-AC02-06CH11357. The use of the PILATUS3 X CdTe 1M detector was supported by the National Science Foundation (NSF) under Grant No. NSF/DMR-1531283.

AUTHOR DECLARATIONS

Conflict of Interest

The authors have no conflicts to disclose.

Author Contributions

Wilarachchige D. C. B. Gunatilleke: Formal analysis (equal); Investigation (equal); Visualization (equal). Mingjian Zhang: Data curation (equal). Winnie Wong-Ng: Data curation (equal); Formal analysis (equal). Peter Zavalij: Data curation (equal). Yu-Sheng Chen: Data curation (equal); Formal analysis (equal). George S. Nolas: Conceptualization (equal); Investigation (equal); Project administration (equal); Supervision (equal); Writing – original draft (equal); Writing – review & editing (equal).

DATA AVAILABILITY

The data that support the findings of this study are available within the article and its supplementary material.

REFERENCES

¹G. A. Jeffrey, in *Inclusion Compounds*, edited by J. L. Atwood, J. E. D. Davies, and D. D. MacNicol (Academic Press, 1984), Vol. 1, p. 135.

²G. S. Nolas, The Physics and Chemistry of Inorganic Clathrates (Springer, 2014),

³G. S. Nolas and G. A. Slack, Am. Sci. 89, 136 (2001).

⁴G. S. Nolas, G. A. Slack, and S. B. Schujman, "Semiconducting clathrates: A phonon glass electron crystal material with potential for thermoelectric applications," in *Semiconductors and Semimetals*, edited by T. M. Tritt (Academic Press, San Diego, 2000), Vol. 69, p. 255.

⁵M. Beekman and G. S. Nolas, J. Mater. Chem. 18, 842 (2008).

⁶G. B. Adams, M. O'Keeffe, A. A. Demkov, O. F. Sankey, and Y.-M. Huang, Phys. Rev. B **49**, 8048 (1994).

⁷K. Moriguchi, S. Munetoh, and A. Shintani, Phys. Rev. B 62, 7138 (2000).

⁸X. Blase, P. Gillet, A. San Miguel, and P. Mélinon, Phys. Rev. Lett. **92**, 21550 (2004)

⁹P. Warrier and C. A. Koh, Appl. Phys. Rev. 3, 040805 (2016).

¹⁰M. H. Phan, G. T. Woods, A. Chaturvedi, S. Stefanoski, G. S. Nolas, and H. Srikanth, Appl. Phys. Lett. **93**, 252505 (2008).

¹¹G. S. Nolas, J. L. Cohn, G. A. Slack, and S. B. Schujman, Appl. Phys. Lett. 73, 178 (1998)

¹²T. Takabatake, K. Suekuni, T. Nakayama, and E. Kaneshita, Rev. Mod. Phys. 86, 669 (2014).

¹³A. Fujiwara, K. Sugimoto, C. H. Shih, H. Tanaka, J. Tang, Y. Tanabe, J. Xu, S. Heguri, K. Tanigaki, and M. Takata, Phys. Rev. B 85, 144305 (2012).

¹⁴M. Beekman, D. Morelli, and G. S. Nolas, Nat. Mater. **14**, 1182 (2015).

- ¹⁵M. A. Avila, K. Suekuni, K. Umeo, H. Fukuoka, S. Yamanaka, and T. Takabatake, Phys. Rev. B 74, 125109 (2006).
- ¹⁶M. Christensen, A. B. Abrahamsen, N. B. Christensen, F. Juranyi, N. H. Andersen, K. Lefmann, J. Andreasson, C. R. H. Bahl, and B. B. Iversen, Nat. Mater. 7, 811 (2008).
- ¹⁷S. Christensen, M. S. Schmøkel, K. A. Borup, G. K. H. Madsen, G. J. McIntyre, S. C. Capelli, M. Christensen, and B. B. Iversen, J. Appl. Phys. 119, 185102 (2016).
- ¹⁸G. S. Nolas, T. J. R. Weakley, J. L. Cohn, and R. Sharma, Phys. Rev. B 61, 3845 (2000).
- ¹⁹B. C. Sales, B. C. Chakoumakos, R. Jin, J. R. Thompson, and D. Mandrus, Phys. Rev. B **63**, 245113 (2001).
- ²⁰M. Christensen, N. Lock, J. Overgaard, and B. B. Iversen, J. Am. Chem. Soc. 128, 15657 (2006).
- ²¹V. Keppens, M. A. McGuire, A. Teklu, C. Laermans, B. C. Sales, D. Mandrus, and B. C. Chakoumakos, Physica B **316**, 95 (2002).
- Zerec, V. Keppens, M. A. McGuire, D. Mandrus, B. C. Sales, and P. Thalmeier, Phys. Rev. Lett. 92, 185592 (2004).
- ²³R. P. Hermann, V. Keppens, P. Bonville, G. S. Nolas, F. Grandjean, G. J. Long, H. M. Christen, B. C. Chakoumakos, B. C. Sales, and D. Mandrus, Phys. Rev. Lett. 97, 017401 (2006).
- ²⁴K. Suekuni, M. A. Avila, K. Umeo, and T. Takabatake, Phys. Rev. B 75, 195210 (2007).
- ²⁵T. Tadano, Y. Gohda, and S. Tsuneyuki, Phys. Rev. Lett. **114**, 095501 (2015).
- ²⁶G. K. H. Madsen, A. Katre, and C. Bera, Phys. Status Solidi A 213, 802 (2016).
- 27. M. Beekman and A. VanderGraaff, J. Appl. Phys. 121, 205105 (2017).
- ²⁸M. Beekman, R. P. Hermann, A. Möchel, F. Juranyi, and G. S. Nolas, J. Phys.: Condens. Matter. 22, 355401 (2010).
- ²⁹K. Biswas, C. W. Myles, M. Sanati, and G. S. Nolas, J. Appl. Phys. **104**, 033535 (2008).
- Martin, G. S. Nolas, H. Wang, and J. Yang, J. Appl. Phys. 102, 103719 (2007).
 E. S. Toberer, L. L. Baranowski, and C. Dames, Annu. Rev. Mater. Res. 42, 179 (2012).
- ³²B. Liu, Y. Liu, C. Zhu, H. Xiang, H. Chen, L. Sun, Y. Gao, and Y. Zhou, J. Mater. Sci. Technol. 35, 833 (2019).
- ³³A. Prokofiev, A. Sidorenko, K. Hradil, M. Ikeda, R. Svagera, M. Waas, H. Winkler, K. Neumaier, and S. Paschen, Nat. Mater. 12, 1096 (2013).
- 34S. M. Kauzlarich, F. Sui, and C. J. Perez, Materials 9, 714 (2016).
- 35C. Cros, M. Pouchard, and P. Hagenmuller, C. R. Hebd. Seances Acad. Sci. 260, 4764 (1965).
- 36J. S. Kasper, P. Hagenmuller, M. Pouchard, and C. Cros, Science 150, 1713 (1965)
- ³⁷A. D. Ritchie, M. B. Johnson, J. F. Niven, M. Beekman, G. S. Nolas, J. Gryko, and M. A. White, J. Phys.: Condens. Matter. 25, 435401 (2013).
- ³⁸S. Stefanoski, C. D. Malliakas, M. G. Kanatzidis, and G. S. Nolas, Inorg. Chem. 51, 8686 (2012).
- ³⁹M. Beekman, E. N. Nenghabi, K. Biswas, C. W. Myles, M. Baitinger, Y. Grin, and G. S. Nolas, Inorg. Chem. 49, 5338 (2010).
- ⁴⁰M. Beekman and G. S. Nolas, Phys. B: Condens. Matter. **383**, 111 (2006).
- ⁴¹G. S. Nolas, J. L. Cohn, and G. A. Slack, Phys. Rev. B. 58, 164 (1998).

- ⁴²G. S. Nolas, M. Kaeser, R. T. Littleton IV, and T. M. Tritt, Appl. Phys. Lett. 77, 1855 (2000).
- ⁴³G. A. Lamberton Jr, R. H. Tedstrom, T. M. Tritt, and G. S. Nolas, J. Appl. Phys. 97, 113715 (2005).
- 44G. S. Nolas, G. Fowler, and J. Yang, J. Appl. Phys. 100, 043705 (2006).
- ⁴⁵G. P. Meisner, D. T. Morelli, S. Hu, J. Yang, and C. Uher, Phys. Rev. Lett. 80, 3551 (1998).
- 46 Certain trade names and company products are mentioned in the text or identified in illustrations in order to adequately specify the experimental procedures and equipment used. In no case does such identification imply recommendation or endorsement by the National Institute of Standards and Technology.
- 47 Bruker, Apex2 (Bruker AXS Inc., Madison, WI, 2010).
- ⁴⁸J. Martin and G. S. Nolas, Rev. Sci. Instrum. **87**, 015105 (2016).
- ⁴⁹A. Czybulka, B. Kuhl, and H.-U. Schuster, Z. Anorg. Allg. Chem. **594**, 23 (1991).
- 50 A. P. Wilkinson, C. Lind, R. A. Young, S. D. Shastri, P. L. Lee, and G. S. Nolas, Chem. Mater. 14, 1300 (2002).
- 51T. Kawaguchi, K. Tanigaki, and M. Yasukawa, Appl. Phys. Lett. 77, 3438 (2000)
- ⁵²Y. Zhang, P. L. Lee, G. S. Nolas, and A. P. Wilkinson, Appl. Phys. Lett. **80**, 2931 (2002)
- ⁵³K. Wei, A. R. Khabibullin, D. Hobbis, W. Wong-Ng, T. Chang, S. G. Wang, I. Levin, Y. S. Chen, L. M. Woods, and G. S. Nolas, Inorg. Chem. 57, 9327 (2018).
- ⁵⁴B. C. Sales, D. Mandrus, and B. C. Chakoumakos, Semiconductors and Semimetals (Academic, New York, 2001). Vol. 70, p. 1.
- 55J. L. Cohn, G. S. Nolas, V. Fessatidis, T. H. Metcalf, and G. A. Slack, Phys. Rev. Lett. 82, 779 (1999).
- ⁵⁶From the Weidemann–Franz relation $\kappa = \kappa_E + \kappa_L$ and the electronic contribution $\kappa_E = L_0 \sigma T$, with the Lorentz number, L_0 , taken to be $2.45 \times 10^{-8} \, \mathrm{V^2 \, K^{-2}}$; therefore, $\kappa \gg \kappa_E$.
- 57 J. E. Graebner, B. Golding, and L. C. Allen, Phys. Rev. B 34, 5696 (1986), and references therein.
- 58C. W. Myles, J. Dong, and O. F. Sankey, Phys. Rev. B 64, 165202 (2001).
- $^{59}C_{\rm p}-C_{\rm V}=KTV(\alpha_{\rm V})^2$, where $\alpha_{\rm V}$ is the volume thermal expansion coefficient experimentally obtained from our T-dependent structural data, V is the unit cell volume, and K is the bulk modulus for α -Sn from Ref. 58, as no K data exist for this new clathrate-I composition.
- ⁶⁰L. Qiu, I. P. Swainson, G. S. Nolas, and M. A. White, Phys. Rev. B 70, 035208 (2004).
- ⁶¹G. S. Nolas, J.-M. Ward, J. Gryko, L. Qiu, and M. A. White, Phys. Rev. B 64, 153201 (2001).
- 62S. Stefanoski, J. Martin, and G. S. Nolas, J. Phys.: Condens. Matter. 22, 485404 (2010)
- ⁶³L. Qiu, M. A. White, Z. Li, J. S. Tse, C. I. Ratcliffe, C. A. Tulk, J. Dong, and O. F. Sankey, Phys. Rev. B 64, 024303 (2001).
- 64 J. S. Tse, J. Phys. Colloq. 48, C1-543-C1-549 (1987).
- 65 J. S. Tse and M. A. White, Phys. Chem. 92, 5006 (1988).
- 66 T. H. K. Barron, J. G. Collins, and G. K. White, Adv. Phys. 29, 609 (1980).
- 67M. Zakrzewski and M. A. White, J. Phys.: Condens. Matter 3, 6703 (1991).